Characterization of Liquid Crystal Polymer (LCP) Material and Transmission Lines on LCP Substrates From 30 to 110 GHz

Dane C. Thompson, *Student Member, IEEE*, Olivier Tantot, Hubert Jallageas, George E. Ponchak, *Senior Member, IEEE*, Manos M. Tentzeris, *Senior Member, IEEE*, and John Papapolymerou, *Senior Member, IEEE*

***Abstract*—Liquid crystal polymer (LCP) is a material that has gained attention as a potential high-performance microwave substrate and packaging material. This investigation uses several methods to determine the electrical properties of LCP for millimeter-wave frequencies. Microstrip ring resonators and cavity resonators are measured in order to characterize the dielectric constant (ϵ_r) and loss tangent ($\tan\delta$) of LCP above 30 GHz. The measured dielectric constant is shown to be steady near 3.16, and the loss tangent stays below 0.0049. In addition, various transmission lines are fabricated on different LCP substrate thicknesses and the loss characteristics are given in decibels per centimeter from 2 to 110 GHz. Peak transmission-line losses at 110 GHz vary between 0.88–2.55 dB/cm, depending on the line type and geometry. These results show, for the first time, that LCP has excellent dielectric properties for applications extending through millimeter-wave frequencies.**

***Index Terms*—Cavity resonator, dielectric characterization, liquid crystal polymer (LCP), loss tangent, millimeter-wave frequencies, ring resonator, transmission-line loss.**

I. Introduction

As frequencies tend to increase for the next generation of wireless applications, the materials and integration techniques in RF systems are experiencing more demanding performance constraints. One example is substrate water absorption, which above 10 GHz can lead to unacceptable losses in elements such as antennas, filters, and transmission lines. Many materials whose losses are small for 2.4- and 5.8-GHz wireless local area networks (LANs) are no longer suitable for 35-GHz satellite, 60-GHz high-bandwidth wireless LANs, 77-GHz vehicular collision avoidance, and 94-GHz military bands to name a few. In addition, consumers are demanding continually better performance for minimal increases in price. New material technologies must be identified that can simultaneously tackle these challenges of performance, frequency and environmental invariance, and cost.

Millimeter-wave systems are designed around two major philosophies: system-on-chip (SoC) and system-on-package (SoP). SoC is a fully integrated design with RF passives and digital and/or optical functions on-wafer [1]. SoP condenses space hungry analog components into a multilayer dielectric material and integrates chips within or on the same dielectric packaging material [2]. For SoC, especially at higher frequencies, gallium arsenide (GaAs) is often required for the high cutoff frequency performance it offers digital transistors and for the low substrate loss it provides analog components. However, GaAs is expensive, and using large areas of the substrate for analog components is not cost effective. Silicon germanium (SiGe) on either CMOS/BiCMOS-grade Si or high-resistivity Si is a lower cost replacement for GaAs for some applications, but it is still a relatively lossy substrate for passive RF components. SoP modules solve the major shortfalls of SoC by providing a low-loss substrate material for the RF passives and a unique space-saving capability for chip integration in or on the substrate.

Still, many of the materials commonly used for SoP microwave circuit construction have shortfalls that limit their implementation for higher frequency applications, such as in the millimeter-wave applications. The industry standard for circuit boards, i.e., FR4, becomes dysfunctional due to prohibitively large losses in the high gigahertz range. Low temperature co-fired ceramic (LTCC) has attractive electrical characteristics, dense multilayer circuit integration, and very good package hermeticity, but the cost is also relatively high [3].

One potential material that could address the needs for wireless systems built across a very wide frequency range is liquid crystal polymer (LCP). The low loss ($\tan\delta = 0.002$–0.004 for $f < 35$ GHz) [5]–[7], near hermetic nature (water absorption <0.04%) [8], and low cost ($\sim$\$5/ft^2 for 2-mil single-clad low-melt LCP) [9] make it appealing for high-frequency designs where excellent performance is required for minimal cost. LCP's low water absorption makes it stable across a wide range of environments by preventing changes in the relative dielectric constant (ϵ_r) and loss tangent ($\tan\delta$). The LCP material processing is still in its infancy, and its materials cost is on the same

Manuscript received November 4, 2003. This work was supported by the National Aeronautics and Space Administration under Contract NCC3-1015, by the National Science Foundation (NSF) under CAREER Award ECS 9984761, by the Georgia Electronic Design Center, and by the Georgia Institute of Technology NSF Packaging Research Center.

D. C. Thompson, M. M. Tentzeris, and J. Papapolymerou are with the School of Electrical and Computer Engineering, Georgia Institute of Technology, Atlanta, GA 30332 USA (e-mail: Dane.Thompson@ece.gatech.edu).

O. Tantot and H. Jallageas are with the Faculté des Sciences, Institut de Recherche en Communications Optiques et Microondes, Université de Limoges, Limoges Cedex 87060, France.

G. E. Ponchak is with the National Aeronautics and Space Administration Glenn Research Center, Cleveland, OH 44135 USA.

Digital Object Identifier 10.1109/TMTT.2004.825738

TABLE I
MATERIAL COMPARISON

	ε_r	tan δ	f_{meas} [GHz]
* FR4	4	0.025	< 10
** LTCC	5.7 - 9.1	0.0012 - 0.0063	< 12
***LCP	2.9 - 3.2	0.002 - 0.0045	< 105

* [4] Typical value shown.
** [4] Values vary by manufacturer (range is shown)
*** From previous literature and this publication

magnitude with those in Table I. However, due to the capability for LCP to do reel-to-reel processing, it is expected that production costs will continue to fall. At the same time, the material's flexibility and relatively low processing temperatures enable applications such as conformal antenna arrays and integration of microelectromechanical system (MEMS) devices such as low-loss RF switches.

In addition, multilayer circuits are possible due to two types of LCP material with different melting temperatures. High melting temperature LCP (315 °C) can be used as core layers, while low melting temperature LCP (290 °C) is used as a bond ply. Thus, vertically integrated designs may be realized similar to those in LTCC. An additional benefit in multilayer LCP builds is the functionality provided by the low dielectric constant. This is useful for vertically integrated designs where the antenna is printed on the top layer of an all-LCP module.

The usage of LCP as a microwave circuit substrate is not a new idea. It has been around in thin-film form since the early 1990s when it was first recognized as a candidate for microwave applications [5], [10], [11]. However, early LCP films would easily tear and were difficult to process. Film uniformity was not acceptable and poor LCP to metal adhesion and failure to produce reliable plated through holes (PTHs) in LCP limited the capabilities for manufacturing circuits on it. Devising and optimizing LCP surface treatments and via drilling and de-smearing techniques were also necessary in order to bring the material to a state where circuits on it could be manufactured with confidence. Much work has focused on methods of improving these fabrication difficulties [12]–[19].

A biaxial die extrusion process was developed [8], [9], [11], which solved the tearing problems by giving the material uniform strength and it also created additional processing benefits. It was discovered that by controlling the angle and rate of LCP extrusion through the biaxial die, the x–y coefficient of thermal expansion (CTE) could be controlled approximately between 0 ppm/°C and 40 ppm/°C. Thus, this unique process can achieve a thermal expansion match in the x–y-plane with many commonly used materials. Table II shows how the transverse CTE of LCP can be made to match both metals and semiconductors used in high-frequency systems.

LCP's z-axis CTE is considerably higher ($\sim$ 105 ppm/°C), but due to the thin layers of LCP used, the absolute z-dimension difference between LCP and a 2-mil-high copper PTH is less than one half-micrometer within a $\pm$100 °C temperature range [20]. This makes z-axis expansion a minimal concern until very thick multilayer modules come into consideration.

It was not until late 2002 that many of the LCP process limitations had been overcome [21], and it has only been available commercially in thin films with single and double copper cladding since December 2001 and June 2003, respectively.[1] Interest has grown quickly in utilizing LCP for higher frequency applications since [22], [23].

Previous literature [5]–[7] has focused on lower frequency characterization of LCP using microstrip ring resonators to extract ϵ_r and $\tan\delta$ up to 34.5 GHz. Additionally, a 50-Ω conductor-backed coplanar waveguide (CBCPW) transmission line on LCP [24] has shown LCP to have low loss from 2 to 110 GHz, and a CPW on LCP [25] has been measured to 50 GHz.

However, broad-band dielectric material characterization at higher frequencies is not a trivial task. Ring resonators provide dielectric information at discrete frequency points at periodic resonant peaks, but substrate thickness, ring diameter, and the dielectric constant of the material under test may all affect the accuracy of the measurement. In addition, at high frequencies where the skin depth approaches the surface roughness of the resonator's metal lines, it becomes difficult to theoretically separate the effects of conductor and dielectric losses.

In this paper, for the first time, a thorough analysis using multiple dielectric characterization methods has been performed in order to provide accurate broad-band dielectric properties (ϵ_r, $\tan\delta$) of LCP for frequencies from 30 to 110 GHz. Microstrip ring resonators of varying diameters and substrate thicknesses, cavity resonators, and a transmission-line method (TL method) have all been used and cross-referenced to accurately determine the broad-band ϵ_r and $\tan\delta$ values for LCP. In addition, coplanar waveguides (CPWs) and microstrip lines, each on varying substrate thicknesses, have been characterized for the first time from 2 to 110 GHz and the losses have been quantified in decibels per centimeter. The transmission line losses across the millimeter-wave range provide a design guide for loss versus frequency of circuits built on LCP substrates. The results of this investigation give a thorough knowledge of LCP dielectric properties and the performance of LCP-based circuits up to millimeter-wave RF systems.

II. MILLIMETER-WAVE (>30 GHz) LCP CHARACTERIZATION

A. Ring Resonator Method

Microstrip ring resonators were initially designed for 2- and 4-mil LCP substrates. The LCP substrates, courtesy of the Rogers Corporation, came double copper clad with 18 μm of electrodeposited copper. The copper surface was first examined using a Wyko optical profilometer, which showed 0.4–0.6-μm rms surface roughness. Unfortunately, accurate $\tan\delta$ extraction using the ring resonator method requires reliable theoretical equations for microstrip conductor losses. With the surface roughness potentially approaching the copper skin depth as low as 12 GHz, an undesirably large surface roughness correction factor would be required in the conductor loss formulas for frequencies above 30 GHz. As a solution, the 18-μm copper was etched off of one side of 2- and 4-mil-high melt temperature LCP core layers. A Karl Suss SB-6 wafer bonder was used to bond a smooth 5-μm rolled copper foil to the bare 2- and 4-mil LCP surfaces with a 1-mil low melting temperature LCP layer

[1] Rogers Corporation, Rogers, CT. [Online]. Available: http://www.rogerscorporation.com/whatsnew.htm

TABLE II
TRANSVERSE COEFFICIENT OF THERMAL EXPANSION COMPARISON

	LCP	Cu	Au	Si	GaAs	SiGe
CTE (ppm/°C)	0-40	16.8	14.3	4.2	5.8	3.4-5

TABLE III
RING RESONATOR CONFIGURATIONS NOTE: ALL DIMENSIONS ARE IN MICROMETERS, EXCEPT FOR "h," WHICH IS IN mils

	Ring Resonator			CBCPW					Microstrip	
	h	r_m	G	S	W	Wg	TL	L	W	L
A	3	1477	80	104	85	276	0	250	104	500
B	3	2947	70	104	85	276	0	250	104	500
C	5	1477	80	104	85	276	0	250	104	500
D	5	2947	70	104	85	276	0	250	104	500
E	5	2683	185	196	85	506	100	150	234	500
F	5	2954	185	196	85	506	100	150	234	500

as the bond layer. As a result of this process modification, the ensuing ring resonators were patterned on 3- and 5-mil LCP substrates. The bonded construction is assumed electrically homogeneous since identical electrical characteristics are listed for high and low melting temperature LCP. Depending on the orientation to the rolled foil's copper grain structure, its rms surface roughness measured between 0.1–0.35 μm. With these values, the surface roughness reaches the copper skin depth at the worst case near 36 GHz, while at the moderate to best case, the roughness would not approach the skin depth until well after 110 GHz.

The ring resonator designs produce an S_{21} with periodic resonant peaks. The extraction of ϵ_r is dependent on the location of the resonant frequencies for a resonator of a given radius, while the $\tan\delta$ extracted is a function of the quality factor (Q) of the peaks.

For each substrate thickness, the desired resonant peaks and corresponding ring radii were devised according to

$$f_o = \frac{nc}{2\pi r_m \sqrt{\varepsilon_{\text{eff}}}} \tag{1}$$

where f_o corresponds to the nth resonant frequency of a ring with mean radius r_m, effective dielectric constant ϵ_{eff}, and c being the speed of light in vacuum [6], [26].

To experiment how sensitive the results would be to the number of resonances, small and large ring diameters were employed for each substrate thickness. The small ring was designed for approximately five resonant peaks and the large one for approximately ten peaks across the 2–110-GHz measured frequency range. A standard microstrip feed could not be used due to the cutoff of most coaxial connectors at 50 GHz. Thus, CBCPW-to-microstrip transitions were included on both ends of the ring resonators so that on-wafer probes rated to 110 GHz could be utilized. The transitions were optimized for frequencies above 30 GHz.

We chose an impedance range between 60–90 Ω for the microstrip and CBCPW lines in our designs. High-impedance lines are desirable in ring resonator designs [27], [28] in order to reduce the dispersion that is common for a microstrip.

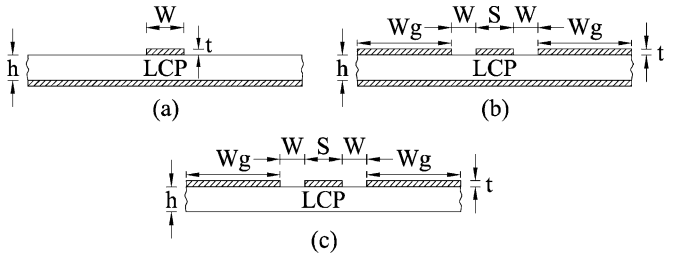

Fig. 1. Transmission-line cross sections for: (a) microstrip, (b) CBCPW, and (c) CPW.

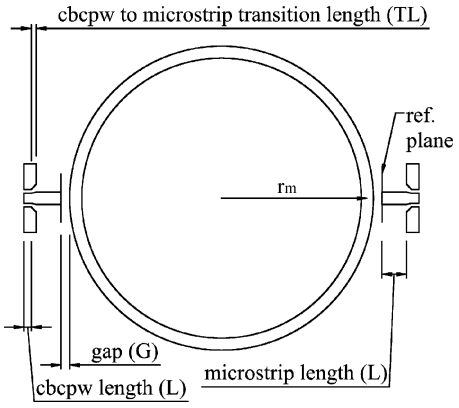

Fig. 2. Microstrip ring resonator configuration diagram.

Simulations using Ansoft HFSS and Flomerics microstrips helped narrow the designs to those shown in Table III. Dimensioning nomenclature for the transmission-line cross sections and ring resonator layout are shown in Figs. 1 and 2.

As shown in Table IV, designs A, B, E, and F have closely matched CBCPW to microstrip impedances, while designs C and D were mismatched to provide a higher impedance for the microstrip portion. Slight mismatches in the design were due to a combination of factors. The probe pitch for the ground–signal–ground (GSG) probes gave dimensional limitations for the $S + 2W$ of the CBCPW, and depending on the substrate thickness, the signal width for CBCPW and microstrip lines of the same impedance were sometimes difficult to match. Thus, a tapered 100-μm transition section was used in some designs. The etching undercut during fabrication also

TABLE IV
RING RESONATOR IMPEDANCES

	CBCPW [Ω]	Microstrip [Ω]
A, B	68	71
C, D	80	91
E, F	60	61

TABLE V
TRL LINES USED IN CBCPW-TO-MICROSTRIP TRANSITION

TRL Lines	Total Length [cm]
Delay 1	1.1924
Delay 2	0.4590
Delay 3	0.2436
Delay 4	0.1838
Delay 5	0.1653
Delay 6	0.1535
Through	0.1000
Reflect Open	0.0500

played a role in the final dimensions. The dimensions shown in Table III are those measured from the fabricated structures. Impedances in Table IV have been calculated with the HP ADS LineCalc software utility using the fabricated dimensions and assuming the manufacturers specification of $\epsilon_r = 2.9$. The microstrip impedances have been taken near the middle of our frequency range (at 60 GHz) due to the $\sim 2\Omega$ variation in calculated microstrip impedance between 30–110 GHz.

To remove the effects of the feeding sections and eliminate the effects of the slight impedance mismatch, a through-reflect-line (TRL) calibration was performed with six delay lines, a through, and an open reflect. HP BASIC and the National Institute of Standards and Technology (NIST), Boulder, CO, Multical software were used in the calibration [29]. A reference plane was set at the edge of the coupling gap to the resonator so that only the response of the resonating ring element (a microstrip ring) was effectively measured. The TRL lines lengths used in the calibration are shown in Table V.

The measurements were done over a 2–110-GHz band using an Agilent 8510XF vector network analyzer (VNA) and Cascade Microtech 250 μm probe pitch GSG 110-GHz probes. The maximum number of frequency points (801) and an averaging factor of 128 were used in the measurement. The 3-dB bandwidth of the resonant peaks was found to be roughly one-hundredth of the frequency at which they occurred. Thus, the 3-dB bandwidth was around 300 MHz for a 30-GHz peak and near 1 GHz for a 100-GHz peak. The measured data points were 135 MHz apart, but post-processing interpolation using MATLAB with an interpolation factor of 15 gave frequency resolution of approximately 10 MHz.

A test was applied to determine if the accuracy of this interpolation method was sufficient. A TRL calibration and re-measurement of a known resonant peak was performed using 801 data points over a 4-GHz band. The results with this 5-MHz resolution were almost identical to that using more sparse data points and interpolation. Following this test, the rest of the measurements were done using broad-band measurement with data interpolation.

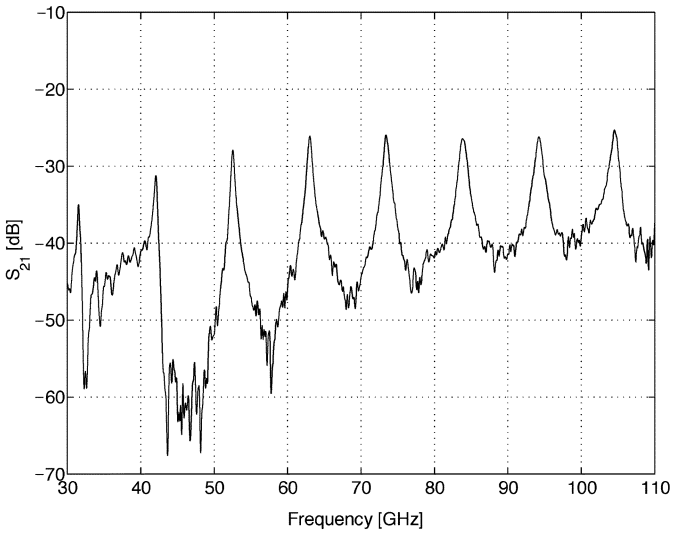

Fig. 3. S_{21} measurement for ring resonator configuration D.

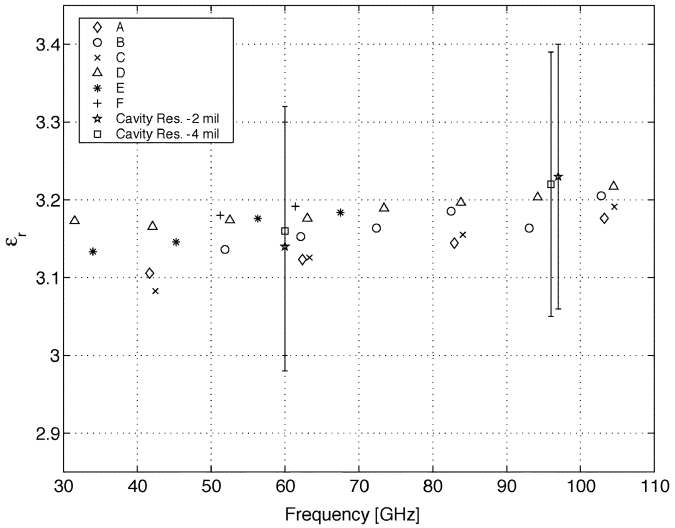

Fig. 4. Extracted dielectric constant using ring resonator designs A–F and cavity resonators with 2- and 4-mil LCP.

One such measurement file is shown in Fig. 3. The extracted ϵ_r values are shown in Fig. 4. ϵ_{eff} and ϵ_r are both obtained using the equations found in [7]. Depending on the geometry, different numbers of resonant peaks were discernible for different designs, and only clearly defined resonant peaks were evaluated. The dielectric constant results vary by less than 2.6% between the six resonator designs in any 10-GHz frequency band and less than 4.3% over the entire 80-GHz band. The results show approximately that $\epsilon_r = 3.16 \pm 0.05$ with a slight increase with increasing frequency. The lowest value observed was 3.083 and the highest was 3.217, but a majority of the data points fell closer to the high end of the spectrum. In ϵ_r data point groupings near 43, 62, and 104 GHz, the approximate average values are 3.13, 3.15, and 3.19, respectively.

The extraction of loss tangent using the ring resonator at such high frequencies has proven more difficult. The ring resonator method gives the total loss at the frequency locations of each resonant peak [6], and subtracting theoretical values for conductor and radiation losses is required to isolate the dielectric

loss (α_d). α_d in nepers per meter may then be inserted into (2) to obtain the results for loss tangent [30].

$$\tan\delta = \frac{\alpha_d \lambda_0 \sqrt{\varepsilon_{\text{eff}}}(\varepsilon_r - 1)}{\pi \varepsilon_r (\varepsilon_{\text{eff}} - 1)} \tag{2}$$

where λ_0 is the free-space wavelength, ϵ_{eff} is the effective dielectric constant, and ϵ_r is the relative dielectric constant.

Accurate theoretical equations for both conductor and radiation losses are a necessity for extracting $\tan\delta$ using the microstrip ring resonator method. However, available conductor loss [31]–[34] and radiation loss [33]–[35] formulas are dated from the 1970s or before and were not meant for describing microstrip characteristics in the tens or hundreds of gigahertz. To the authors' knowledge, no analytical formulas are available, which are optimized for describing conductor and radiation losses in a microstrip line from 30 to 110 GHz.

Four microstrip conductor loss formulas were investigated and found to differ significantly. As an example, the theoretical conductor losses on the microstrip geometry on 3-mil LCP (see Section III) differed by approximately 0.74 dB/cm at 110 GHz from highest [34] to lowest [33]. The conductor-loss equation used in a previous LCP material characterization [7] was found to use an incorrect formula for conductor loss [31], which was later corrected in [32]. This would lead to an artificially high extracted loss tangent, which could explain why values for $\tan\delta$ similar to 0.0038 were reported at 10 GHz, while 0.002–0.003 are the values at 10 GHz reported by LCP suppliers Rogers Corporation and W. L. Gore, Elkton, MD, respectively. Sorting out the available theoretical formulas, the combination that gave us reasonable values for extracted loss tangent came from [34] for conductor loss and using 0.35 μm (maximum measured) for our rms surface roughness.

Two of the three radiation loss formulas tested [34], [35], including the one used in [7], give radiation loss curves with unreasonable f^2 increases at frequencies past 30 GHz. In fact, the theoretical radiation losses from these equations give values higher than the total measured loss past approximately 80 GHz. The third radiation loss formula, found in [33] (originally from [36]), is the only one tested that did not diverge to unreasonable levels in our measured frequency band, and it is used in our analysis.

The loss tangent is plotted in Fig. 5 with and without subtracting the radiation loss for an open-ended microstrip from [36]. This radiation loss was multiplied by a factor of two to account for the two open microstrip discontinuities. Radiation from the ring elements was neglected since these are continuous features that are poor radiators on such thin substrates.

The ring resonator plot with the radiation losses subtracted gives a good approximation of the values found by the cavity resonator method. It shows values between 0.003–0.004 with the exception of one outlier near 93 GHz.

B. Cavity Resonator Method

With the aim of verifying the dielectric properties measured by other methods, a resonant cavity method has been used for permittivity and loss-tangent measurements. This technique permits an accurate measurement without preparation of the sample (no cutting, polishing, or metallization) and it avoids any important theoretical approximations.

The sample is inserted between the two halves of a cylindrical cavity excited in the $\text{TE}_{01,2q+1}$ mode. The interior diameter of the cavity determines the frequency band in which, for a given sample, the measurements can be made. Two cavities with resonant frequencies near 60 and 94 GHz have been used. The test geometries are shown in Figs. 6 and 7.

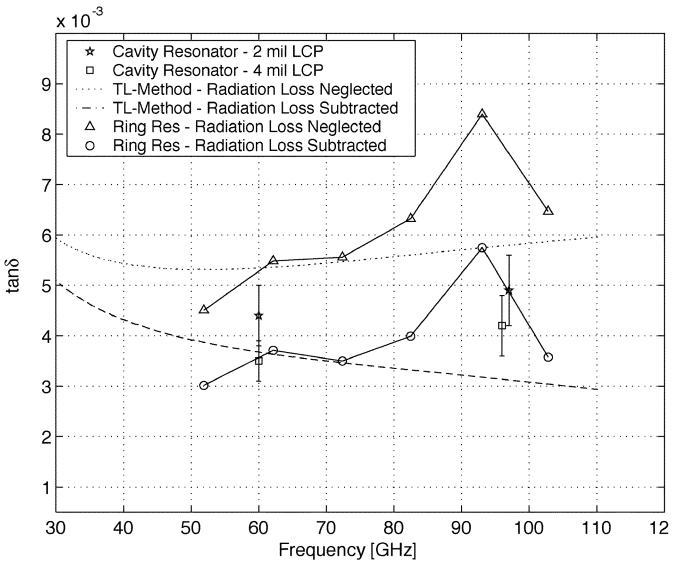

Fig. 5. LCP loss tangent versus frequency for 2- and 4-mil substrate thicknesses measured with the cavity resonator method. Results for the ring resonator method and the TL method on 3-mil LCP substrates are shown with and without subtracting radiation loss.

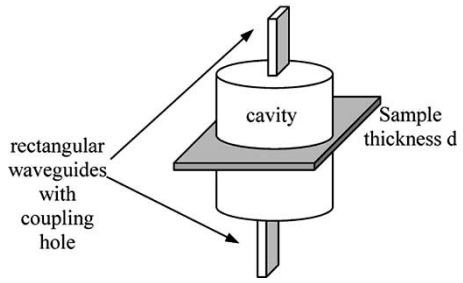

Fig. 6. Cavity resonator diagram.

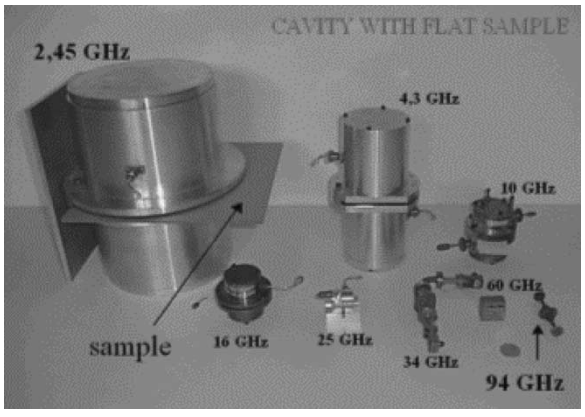

Fig. 7. Cavity resonators for different measurement frequencies.

TABLE VI
SUMMARY OF REPORTED LCP MATERIAL PROPERTIES

Source	f [GHz]	ε_r	tan δ [10^{-3}]
Rogers	10	2.9	2
W. L. Gore	10	3.0	3
[5]	6.97 - 34.66	3.07 - 3.18	-
[6]	3.85 - 34.45	3.00 - 3.04	3.4 - 2.7
This paper	31.53 - 104.60	3.16 ± 0.05	4 at 60 GHz, 4.5 at 97 GHz

Using two of the $\mathrm{TE}_{01,1}$ or 3 or 5 modes, the electrical field is parallel to the dielectric plane and has negligible (practical zero) values close to the gap between the dielectric specimen and the wall of the cavity. The larger dimension of the substrate must be chosen higher than the interior diameter of the cavity ($\phi_c = 7.8$ mm at 60 GHz and 5 mm at 94 GHz) and the thickness less than 0.5 mm at 60 GHz and 0.3 mm at 94 GHz to minimize the radiation in the gap between the two halves of the cavity. In such a configuration, the resonant frequency and quality factor of the $\mathrm{TE}_{01,2q+1}$ mode can be computed exactly. Thanks to an iterative computation, the complex permittivity of the sample can be extracted from the resonant frequency and quality factor. First, the measurement with a VNA of the resonant frequencies of two $\mathrm{TE}_{01,2q+1}$ modes (e.g., TE_{013} and TE_{015}) is necessary to adjust the interior dimensions of the cavity taken into account during computations. The loaded quality factor of one of these modes is used to compute the power losses due to the metallic walls. Only the measurement of the resonant frequency and loaded quality factor of the cavity loaded with a sample is then necessary to determine the permittivity and loss tangent of the substrate [37]. The uncertainties of the quality factors, resonant frequencies, and coupling (through $|S_{21}|$ at the resonant frequency) are reflected in the uncertainties shown for ε_r and $\tan\delta$ of the 2- and 4-mil LCP substrates (Figs. 4 and 5). These error tolerances are due to uncertainties on the cavity dimensions (Δr on radius and ΔH on the height) and on the uncertainty of the sample thickness Δd.

The cavity ε_r results match those of the ring resonators well within the cavity measurement's error tolerance. In regards to $\tan\delta$, the cavity resonator results are our benchmark for accuracy. The values for $\tan\delta$ fall roughly between 0.0035–0.0045 at 60 GHz and 0.0042–0.0049 near 97 GHz (97 GHz is the perturbed cavity resonant frequency with the 2-mil LCP sample inserted).

C. TL Method

Instead of using a ring resonator for the extraction of total loss, a TRL transmission-line calibration can be used to provide the total loss for use in loss-tangent extraction. However, instead of measuring the loss data at widely spaced resonant frequencies, the TRL total loss is at every frequency point in the calibration. The theoretical conductor and radiation losses can be subtracted by curve matching the total loss plot with a smoothed spline and using the same method as described above. The dielectric loss can then be inserted into (2) to retrieve the loss tangent.

As seen in Fig. 5, the loss-tangent values from the TL method settle close to the range defined with the cavity and ring resonators. However, a higher value than expected is seen at the lower end of our measurement spectrum and a slight decrease in loss tangent is observed in the case where radiation losses are subtracted. The discrepancies are likely due to the approximations in conductor and radiation losses. Despite this, the loss tangent for either line in the TL method do not vary by more than 0.002 over the 80-GHz band of measurement (30–110 GHz) and the plot with radiation loss subtracted is a good indicator of the magnitude of dielectric loss.

D. Summary of LCP Material Properties

A summary of previous LCP material characterization, as well as that extended by this paper, are shown in Table VI. In this table, we show the average loss-tangent values for the cavity resonator measurements of the 2- and 4-mil-thick LCP substrates only since these are the most accurate for determining $\tan\delta$ at such high frequencies. The values we measured for ϵ_r are slightly higher than the others shown in Table VI. However, our frequency range is higher and it is shown above that ϵ_r for LCP may increase slightly with frequency. If a linear regression is fitted through the data in Fig. 4 with a slope of 0.12%, the data in this paper would predict an ε_r of 3.1 at 10 GHz, which agrees well with the reported values. Furthermore, the measured value of ε_r at 30 GHz, i.e., 3.12, in this paper agrees with the value in [5], but whereas the wide-band measurements in this paper show an increase in ε_r with frequency, the narrow-band measurements in [5] predict no frequency dependence. As a test, a potential $\pm 10\%$ variation in substrate thickness was investigated in our calculation of ϵ_r, but this modification only results in a change of the extracted ϵ_r by ± 0.02. The loss-tangent values shown in Table VI from this paper are higher than those previously reported, but again, loss tangent is shown in Fig. 5 to be frequency dependent. If only the ring resonator and cavity data in Fig. 5 are used, the loss tangent at 30 GHz is predicted to be approximately 0.0032, which agrees with the value in [6].

III. TRANSMISSION-LINE MILLIMETER-WAVE PERFORMANCE

All transmission-line measurements were done with TRL measurements containing between 4–6 delay lines. The same hardware and software as above was used for all measurements. The dimensions shown are those of the actual fabricated circuits after etching. Undercut of the 5-μm copper foil was measured with a Wyko optical profilometer to be 5 μm, while that of the 18-μm copper had an average value of 13 μm. These values were added or subtracted uniformly to the design dimensions to obtain those given in Tables VII and VIII. The design, fabrication, and measurement of the lines in this section were performed before the dielectric characterization so $\epsilon_r = 2.9$ was used in the initial design process. The Z_0

TABLE VII
CPW CONFIGURATIONS MEASURED LPB: LOSSY POSTER BOARD. HP: HOLLOW PLASTIC. LLF: LOW LOSS FOAM

h [mil]	S [μm]	W [μm]	W_g [μm]	Z_0 [Ω]	Type of Dielectric Spacer	Sets Meas.	Attn. at 110 GHz [dB/cm]
2	221	91	591	83	LPB	1	2.06
4	209	98	561	81	LPB	1	1.80
8	193	104	520	80	LPB	1	1.52
2	221	91	591	83	HP	2	0.96
4	209	98	561	81	HP	2	1.11
8	193	104	520	80	HP	2	1.19
2	221	91	591	83	LLF	3	0.88
4	209	98	561	81	LLF	3	1.08
8	193	104	520	80	LLF	3	1.04

TABLE VIII
MICROSTRIP CONFIGURATIONS MEASURED W_D: DESIGN WIDTH. W: FABRICATED MICROSTRIP WIDTH. $*$: PATTERNED FROM 2- AND 4-mil SUBSTRATE DESIGNS

h [mil]	W_D [μm]	W [μm]	t [μm]	Z_0 [Ω]	Sets Meas.	Attn. at 110 GHz [dB/cm]
2	114	88	18	56	3	2.55
3	*	104	5	68	1	1.94
4	244	218	18	52	4	1.62
5	*	104	5	88	1	1.47
5	*	234	5	59	1	1.39

values in Tables VII and VIII were calculated with the HP ADS LineCalc utility using $\epsilon_r = 3.16$ (from this paper) and the fabricated dimensions.

A. CPWs

CPWs do not have a backside ground plane, but are assumed to have an electrically infinite distance of free space beneath the substrate. However, when performing on-wafer measurements, the sample is usually forced to be in contact with a metal chuck. To overcome this limitation, an electrically thick dielectric spacer must be used between the CPW and chuck. Initially the measurements were tried on a piece of foam poster board, then on a piece of internally corrugated hollow plastic, and finally on a low-loss dielectric spacer from Cuming Microwave, Avon, MA. All of the spacers were from 1/8- to 3/16-in thick. Simulations calculated this thickness to effectively isolate the CPW from the chuck metallization, thus avoiding parasitic microstrip moding. The low-loss dielectric spacer is called C-Stock RH-5, which has $\epsilon_r = 1.09$ and $\tan\delta = 0.0004$ at 5 GHz. For each different spacer, interesting phenomena arose that warranted further testing. Together the three are able to accurately characterize the expected performance of CPW lines.

Due to LCP's low dielectric constant, 50-Ω CPW lines require signal widths and gapwidths far too large to measure with 110-GHz probes. The dimensions selected are based on the probe pitch and on easily fabricated linewidths and gapwidths. The resulting impedances are in the range near 80 Ω. A summary of the circuits measured and the peak attenuation values are shown in Table VII.

Measuring the CPW lines on the lossy poster board gave the cleanest attenuation curves, but it resulted in inaccurately high attenuation values. The results are shown in Fig. 8. In addition, the lines on the thinnest LCP substrate (2-mil) had the greatest loss since this is the configuration that allows the greatest amount of field interaction with the lossy spacer below. Ideally, with a lossless spacer, the 2-mil substrate should be the configuration with the least loss since it would have the least interaction with the LCP substrate and more field lines passing through "free space" on the underside.

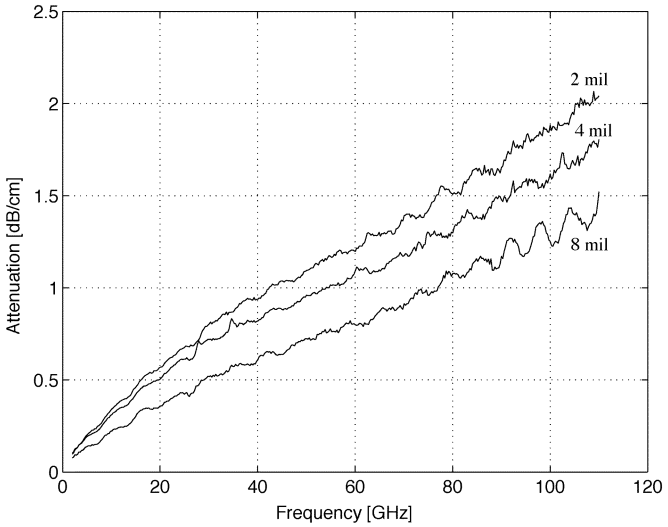

Fig. 8. CPW total measured loss on a lossy poster-board spacer.

The hollow plastic spacer measurements show significantly lower loss in Fig. 9, but large oscillations are seen in the extracted loss data past 70 GHz. The structure of the spacer has waveguide-shaped dielectric channels beneath the thin plastic surface. The dimensions of these channels are consistent with a

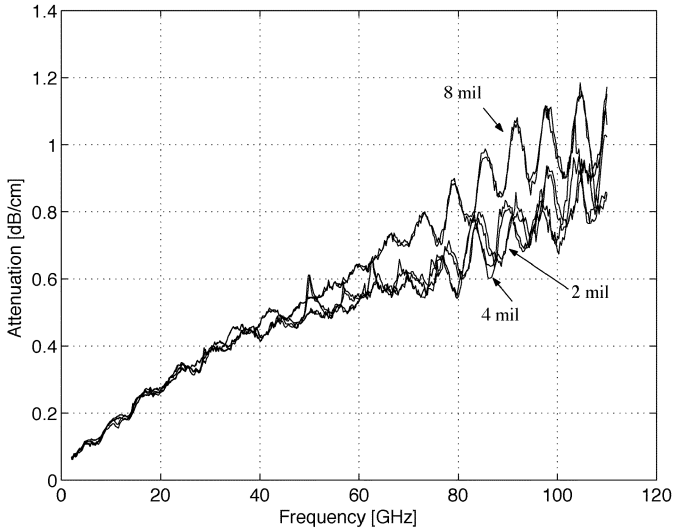

Fig. 9. CPW total measured loss on a hollow plastic spacer.

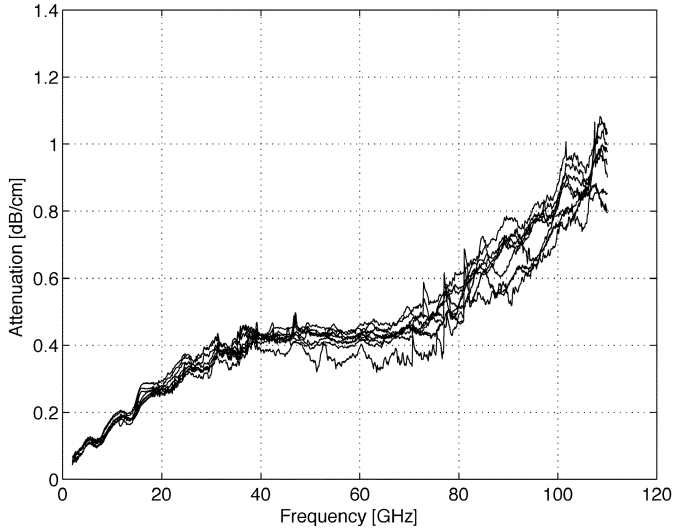

Fig. 10. CPW total measured loss on a low loss foam spacer.

waveguide cutoff frequency near where the oscillations begin to occur. It is expected that these channels could have supported dielectric waveguide modes, resulting in the oscillatory responses shown. However, the loss trend is still easily deciphered and the peak loss level at 110 GHz has values below 1.2 dB/cm.

The low-loss foam spacer in Fig. 10 shows considerable more jitter, a flattening of attenuation in the 40–70-GHz range, and almost indistinguishable attenuation levels between the three substrate thicknesses. The jitter in the measurement can be explained by the surface of the spacer. It is a rigid, but very porous surface that is not uniform or homogenous. The size of the foam cells are on the order of the size of the transmission-line features, which introduces foam cell boundaries to the transmission line along its entire length. Though it performs very well in overall loss levels, the porous surface makes tidy loss plots impossible. The close bunching of the loss characteristics shows that there is minimal interaction with lossy material beneath the LCP. The nine measurement sets are plotted without labeling due to their very close proximity and minimal difference in performance. It

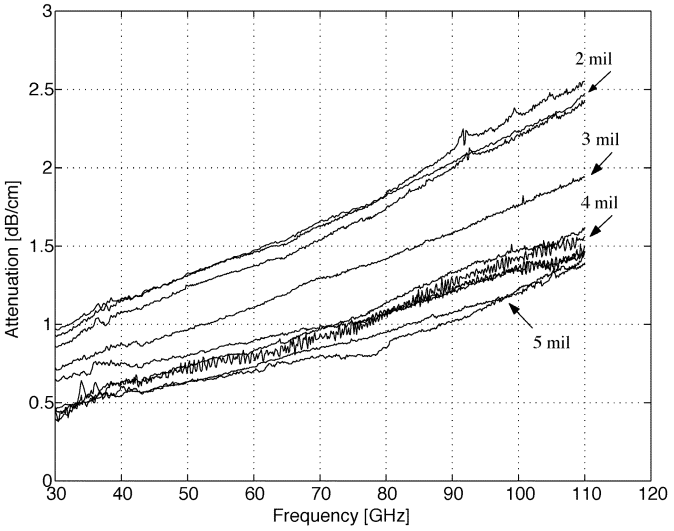

Fig. 11. Microstrip line losses on LCP substrates of 2–5 mil.

is seen that CPW lines on LCP are capable of peaking with loss less than 1 dB/cm up to 110 GHz.

B. Microstrip Lines

Microstrips were designed with masks of $W = 114\ \mu$m for a 2-mil substrate and $W = 244\ \mu$m for a 4-mil substrate in order to obtain 50-Ω lines. These designs were later also patterned on 3- and 5-mil substrates. The 2- and 4-mil substrates were patterned on the 18-μm standard copper, while those on 3- and 5-mil substrates were patterned on the 5-μm rolled copper foil. Due to the undercut and dielectric-constant change to 3.16, the characteristic impedance of the microstrips initially designed for 50 Ω varied by up to 6 Ω. The plots have been suppressed below 30 GHz since the CBCPW-to-microstrip transition is not optimized below this frequency and the loss plot there is somewhat erratic. The fabricated lines had varying impedance values from 52 to 88 Ω. The lines on 2- and 4-mil substrates were measured on several physically different sets of TRL lines. The spread in the attenuation levels is up to 0.15 dB/cm for a single design on a given substrate thickness (for 2- and 4-mil designs). This can be attributed to etching differences and imperfections in the fabrication of the TRL sets and also to measurement errors.

The results in Fig. 11 show that loss decreases with increasing substrate thickness and that microstrip peak loss values are between 1.39–2.55 dB/cm at 110 GHz.

IV. Conclusion

The dielectric properties of LCP and the performance of various planar transmission lines on LCP substrates have been characterized up to 110 GHz. Ring resonator and cavity resonator results show $\epsilon_r = 3.16 \pm 0.05$ from 31.53 to 104.60 GHz and $\tan\delta < 0.0049$ up to 97 GHz. Broad-band ϵ_r extraction was found to be reliable using both ring and cavity resonators, but the cavity resonator measurement is the most accurate for loss-tangent extraction at millimeter-wave frequencies. Transmission lines of various impedances and types on different LCP substrate thicknesses show maximum

attenuation of 0.88–2.55 dB/cm at 110 GHz. LCP is shown to have very attractive qualities as a high-performance low-cost substrate and as a packaging material for numerous applications throughout the millimeter-wave frequency spectrum.

ACKNOWLEDGMENT

The authors would like to thank C. Roseen and C. Murphy, both of the Rogers Corporation, Rogers CT, for supplying the LCP material and for their helpful correspondence regarding our processing. In addition, the authors are grateful to M. Janezic, National Institute of Standards and Technology (NIST), Boulder, CO, for discussion and testing of LCP properties at lower frequencies than are reported in this paper.

REFERENCES

[1] A. Matsuzawa, "RF-SoC—Expectations and required conditions," *IEEE Trans. Microwave Theory Tech.*, vol. 50, pp. 245–253, Jan. 2002.

[2] K. Lim, S. Pinel, M. F. Davis, A. Sutono, C.-H. Lee, D. Heo, A. Obatoynbo, J. Laskar, M. Tentzeris, and R. Tummala, "RF-SOP for wireless communications," *IEEE Microwave Mag.*, vol. 3, pp. 88–99, Mar. 2002.

[3] T. Kutilainen. (2003, May) Ceramic interconnect initiative. NextGen 2003, LTCC. [Online]. Available: http://www.imaps.org/cii/NextGen2003.pdf, slides 42 and 43

[4] L. Devlin, G. Pearson, J. Pittock, and B. Hunt, "RF and microwave component development in LTCC," in *IMAPS Nordic 38th Annu. Conf.*, Sept. 2001, [Online]. Available: http://www.plextek.com/papers/nordic.pdf.

[5] K. Jayaraj, T. E. Noll, and D. R. Singh, "RF characterization of a low cost multichip packaging technology for monolithic microwave and millimeter wave integrated circuits," in *URSI Int. Signals, Systems, and Electronics Symp.*, Oct. 1995, pp. 443–446.

[6] G. Zou, H. Gronqvist, P. Starski, and J. Liu, "High frequency characteristics of liquid crystal polymer for system in a package application," in *IEEE 8th Int. Advanced Packaging Materials Symp.*, Mar. 2002, pp. 337–341.

[7] G. Zou, H. Gronqvist, J. P. Starski, and J. Liu, "Characterization of liquid crystal polymer for high frequency system-in-a-package applications," *IEEE Trans. Adv. Packag.*, vol. 25, pp. 503–508, Nov. 2002.

[8] B. Farrell and M. St. Lawrence, "The processing of liquid crystalline polymer printed circuits," in *IEEE Electronic Components and Technology Conf.*, May 2002, pp. 667–671.

[9] C. Murphy, private communication, Jan. 2004.

[10] E. C. Culbertson, "A new laminate material for high performance PCBs: Liquid crystal polymer copper clad films," in *IEEE Electronic Components and Technology Conf.*, May 1995, pp. 520–523.

[11] K. Jayaraj, T. E. Noll, and D. R. Singh, "A low cost multichip packaging technology for monolithic microwave integrated circuits," *IEEE Trans. Antennas Propagat.*, vol. 43, pp. 992–997, Sept. 1995.

[12] C. Khoo, B. Brox, R. Norrhede, and F. Maurer, "Effect of copper lamination on the rheological and copper adhesion properties of a thermotropic liquid crystalline polymer used in PCB applications," *IEEE Trans. Comp., Packag, Manufact., Technol.*, vol. 20, pp. 219–226, July 1997.

[13] T. Suga, A. Takahashi, K. Saijo, and S. Oosawa, "New fabrication technology of polymer/metal lamination and its application in electronic packaging," in *IEEE 1st Int. Polymers and Adhesives in Microelectronics and Photonics Conf.*, Oct. 2001, pp. 29–34.

[14] X. Wang, L. Lu, and C. Liu, "Micromachining techniques for liquid crystal polymer," in *14th IEEE Int. MEMS Conf.*, Jan. 2001, pp. 21–25.

[15] K. Brownlee, S. Bhattacharya, K. Shinotani, C. P. Wong, and R. Tummala, "Liquid crystal polymers (LCP) for high performance SOP applications," in *8th Int. Adv. Packag. Materials Symp.*, Mar. 2002, pp. 249–253.

[16] J. Kivilahti, J. Liu, J. E. Morris, T. Suga, and C. P. Wong, "Panel-size component integration (PCI) with molded liquid crystal polymer (LCP) substrates," in *IEEE Electronic Components and Technology Conf.*, May 2002, pp. 955–961.

[17] T. Suga, A. Takahashi, M. Howlander, K. Saijo, and S. Oosawa, "A lamination technique of LCP/Cu for electronic packaging," in *2nd Int. IEEE Polymers and Adhesives in Microelectronics and Photonics Conf.*, June 2002, pp. 177–182.

[18] T. Zhang, W. Johnson, B. Farrell, and M. St. Lawrence, "The processing and assembly of liquid crystalline polymer printed circuits," presented at the *Int. Microelectronics Symp.*, 2002.

[19] L. Chen, M. Crnic, L. Zonghe, and J. Liu, "Process development and adhesion behavior of electroless copper on liquid crystal polymer (LCP) for electronic packaging application," *IEEE Trans. Electron. Packag. Manufact.*, vol. 25, pp. 273–278, Oct. 2002.

[20] *Modern Machine Shop Online*. [Online]. Available: http://www.mmsonline.com/articles/030107.html

[21] PMTEC LCP Materials Symp., Huntsville, AL, Oct. 29, 2002.

[22] H. Kanno, H. Ogura, and K. Takahashi, "Surface mountable liquid crystal polymer package with vertical via transition compensating wire inductance up to V-band," in *IEEE MTT-S Int. Microwave Symp. Dig.*, vol. 2, June 2003, pp. 1159–1162.

[23] M. F. Davis, S.-W. Yoon, S. Pinel, K. Lim, and J. Laskar, "Liquid crystal polymer-based integrated passive development for RF applications," in *IEEE MTT-S Int. Microwave Symp. Dig.*, vol. 2, June 2003, pp. 1155–1158.

[24] D. Thompson, P. Kirby, J. Papapolymerou, and M. M. Tentzeris, "W-band characterization of finite ground coplanar transmission lines on liquid crystal polymer (LCP) substrates," in *IEEE Electronic Components Technology Conf.*, May 2003, pp. 1652–1655.

[25] Z. Wei and A. Pham, "Liquid crystal polymer (LCP) for microwave/millimeter wave multi-layer packaging," in *IEEE MTT-S Int. Microwave Symp. Dig.*, vol. 3, June 2003, pp. 2273–2276.

[26] L. Hsieh and K. Chang, "Equivalent lumped elements G, L, C, and unloaded Q's of closed- and open-loop ring resonators," *IEEE Trans. Microwave Theory Tech.*, vol. 50, pp. 453–460, Feb. 2002.

[27] I. Wolff and N. Knoppik, "Microstrip ring resonator and dispersion measurement on microstrip lines," *Electron. Lett.*, vol. 7, no. 26, pp. 779–781, Dec. 1971.

[28] J. Frey, *Microwave Integrated Circuits*. Dedham, MA: Artech House, 1975, p. 20.

[29] R. B. Marks, "A multiline method of network analyzer calibration," *IEEE Trans. Microwave Theory Tech.*, vol. 39, pp. 1205–1215, Dec. 1991.

[30] D. M. Pozar, *Microwave Engineering*, 2nd ed. New York: Wiley, 1998, p. 163.

[31] R. A. Pucel, D. J. Massé, and C. P. Hartwig, "Losses in microstrip," *IEEE Trans. Microwave Theory Tech.*, vol. MTT-16, pp. 342–350, June 1968.

[32] ——, "Correction to 'Losses in microstrip'," *IEEE Trans. Microwave Theory Tech.*, vol. MTT-16, p. 1064, Dec. 1968.

[33] B. C. Wadell, *Transmission Line Design Handbook*. Norwood, MA: Artech House, 1991, pp. 93–99.

[34] K. C. Gupta, R. Garg, I. Bahl, and P. Bhartia, *Microstrip Lines and Slotlines*, 2nd ed. Norwood, MA: Artech House, 1996, pp. 108–109.

[35] L. J. van der Pauw, "The radiation of electromagnetic power by microstrip configurations," *IEEE Trans. Microwave Theory Tech.*, vol. 25, pp. 719–725, Sept. 1977.

[36] M. D. Abouzahra and L. Lewin, "Radiation from microstrip discontinuities," *IEEE Trans. Microwave Theory Tech.*, vol. MTT-27, pp. 722–723, Aug. 1979.

[37] P. Guillon and Y. Garault, "Complex permittivity of MIC substrate," *AEU*, pp. 102–104, 1981.

Dane C. Thompson (S'98) was born in Sacramento, CA, in February 1979. He received the B.S. and M.S. degrees in electrical engineering from Santa Clara University, Santa Clara, CA, in 2001 and 2002 respectively, and is currently working toward the Ph.D. degree in electrical and computer engineering at the Georgia Institute of Technology, Atlanta.

His research involves the processing and use of LCP as a high-performance dielectric substrate and packaging material. He is currently researching the utilization of LCP for vertically integrated RF front-ends, for electrical and MEMS packaging, and for dual-frequency dual-polarization multilayer conformal antennas.

Olivier Tantot was born in Bordeaux, France, in August 1965. He received the Doctorat degree from the Université de Limoges, Limoges, France, in 1994.

He is currently an Assistant Professor with the Institut de Recherche en Communications Optiques et Microondes (IRCOM), Université de Limoges. At the end of 1994, he joined the microwave circuits and devices team. His research interests concern the development of new methods of microwave characterization of materials and thin films.

Hubert Jallageas was born in Saint Victurnien, France, in 1947. He received the Master degree from the Université de Limoges, Limoges, France, in 1969.

He is currently an Electronics and Microwave Measurement Engineer with the Institut de Recherche en Communications Optiques et Microondes (IRCOM), Université de Limoges. He joined the microwave circuits and devices team at its creation. His research concerns the development of new measurement devices in the millimeter-wave domain.

George E. Ponchak (S'82–M'83–SM'97) received the B.E.E. degree from Cleveland State University, Cleveland, OH, in 1983, the M.S.E.E. degree from Case Western Reserve University, Cleveland, OH, in 1987, and the Ph.D. degree in electrical engineering from The University of Michigan at Ann Arbor, in 1997.

In 1983, he joined the staff of the Communication Technology Division, National Aeronautics and Space Administration (NASA) Glenn Research Center, Cleveland, OH, where he is currently a Senior Research Engineer. From 1997 to 1998 and 2000 to 2001, he was a Visiting Lecturer with Case Western Reserve University. He has authored and coauthored over 90 papers in refereed journals and symposia proceedings. His research interests include the development and characterization of microwave and millimeter-wave printed transmission lines and passive circuits, multilayer interconnects, uniplanar circuits, microwave microelectromechanical (MEMS) components, and microwave packaging. He is responsible for the development of GaAs, InP, and SiGe MMICs for space applications.

Dr. Ponchak is a senior member of the IEEE Microwave Theory and Techniques Society (IEEE MTT-S) and a member of the International Microelectronics and Packaging Society (IMAPS). He was the recipient of the Best Paper of the ISHM'97 30th International Symposium on Microelectronics Award. He was editor of a Special Issue on Si MMICs of the IEEE TRANSACTIONS ON MICROWAVE THEORY AND TECHNIQUES. He founded the IEEE Topical Meeting on Silicon Monolithic Integrated Circuits in RF Systems and served as its chair in 1998 and 2001 and its digest editor in 2000 and 2003. In addition, he has chaired many IEEE MTT-S International Microwave Symposium workshops and special sessions. He is a member of the IEEE MTT-S International Microwave Symposium (IMS) Technical Program Committee (TPC) on Transmission Line Elements and serves as its chair. He is a member of the IEEE MTT-S Administrative Committee (AdCom) Membership Services Committee.

Manos M. Tentzeris (SM'03) received the Diploma degree in electrical and computer engineering from the National Technical University of Athens, Athens, Greece, in 1992, and the M.S. and Ph.D. degrees in electrical engineering and computer science from The University of Michigan at Ann Arbor, in 1993 and 1998, respectively.

He is currently an Associate Professor with School of Electrical and Computer Engineering, Georgia Institute of Technology, Atlanta. During the summer of 2002, he was a Visiting Professor with the Technical University of Munich, Munich, Germany. He has authored or coauthored over 120 papers in refereed journals and conference proceedings and six book chapters. He has helped develop academic programs in highly integrated packaging for RF and wireless applications, microwave MEMs, SOP-integrated antennas and adaptive numerical electromagnetics (FDTD, multiresolution algorithms). He is the Georgia Tech NSF-Packaging Research Center Associate Director for RF Research and the RF Alliance Leader. He is also the Leader of the Novel Integration Techniques Sub-Thrust of the Broadband Hardware Access Thrust of the Georgia Electronic Design Center (GEDC) of the State of Georgia.

Dr. Tentzeris is member of the Technical Chamber of Greece. He was the 1999 Technical Program co-chair of the 54th ARFTG Conference, Atlanta, GA. He is the vice-chair of the RF Technical Committee (TC16) of the IEEE Components, Packaging, and Manufacturing Technology (CPMT) Society. He was the recipient of the 2003 IEEE CPMT Outstanding Young Engineer Award, the 2002 International Conference on Microwave and Millimeter-Wave Technology Best Paper Award (Beijing, China), the 2002 Georgia Tech-Electrical and Computer Engineering (ECE) Outstanding Junior Faculty Award, the 2001 ACES Conference Best Paper Award, the 2000 NSF CAREER Award, and the 1997 Best Paper Award, International Hybrid Microelectronics and Packaging Society.

John Papapolymerou (S'90–M'99–SM'04) received the B.S.E.E. degree from the National Technical University of Athens, Athens, Greece, in 1993, and the M.S.E.E. and Ph.D. degrees from The University of Michigan at Ann Arbor, in 1994 and 1999, respectively.

From 1999 to 2001, he was a faculty member with the Department of Electrical and Computer Engineering, University of Arizona, Tucson. During the summers of 2000 and 2003, he was a Visiting Professor with The University of Limoges, Limoges, France. In August 2001, he joined the School of Electrical and Computer Engineering, Georgia Institute of Technology, Atlanta, where he is currently an Assistant Professor. He has authored or coauthored over 70 publications in peer reviewed journals and conferences. His research interests include the implementation of micromachining techniques and microelectromechanical system (MEMS) devices in microwave, millimeter-wave, and terahertz circuits and the development of both passive and active planar circuits on Si and GaAs for high-frequency applications.

Dr. Papapolymerou was the recipient of the 2002 National Science Foundation (NSF) CAREER Award, the Best Paper Award presented at the 3rd IEEE International Conference on Microwave and Millimeter-Wave Technology (ICMMT2002), Beijing, China (August 17–19, 2002), and the 1997 Outstanding Graduate Student Instructional Assistant Award presented by the American Society for Engineering Education (ASEE), The University of Michigan Chapter.